

Supplementary Information

Helper Lipid Structure Influences Protein Adsorption and Delivery of Lipid Nanoparticles to Spleen and Liver

Rui Zhang^{1,#}, Rakan El-Mayta^{1,#}, Timothy J. Murdoch², Claude C. Warzecha³, Margaret M. Billingsley¹, Sarah J. Shepherd¹, Ningqiang Gong¹, Lili Wang³, James M. Wilson³, Daeyeon Lee², Michael J. Mitchell^{1,4,5,6,7,*}

¹Department of Bioengineering, University of Pennsylvania, Philadelphia, PA, 19104

²Department of Chemical and Biomolecular Engineering, University of Pennsylvania, Philadelphia, PA, 19104

³Gene Therapy Program, Perelman School of Medicine, University of Pennsylvania, Philadelphia, PA, 19104

⁴Abramson Cancer Center, Perelman School of Medicine, University of Pennsylvania, Philadelphia, PA, 19104

⁵Institute for Immunology, Perelman School of Medicine, University of Pennsylvania, Philadelphia, PA, 19104

⁶Cardiovascular Institute, Perelman School of Medicine, University of Pennsylvania, Philadelphia, PA, 19104

⁷Institute for Regenerative Medicine, Perelman School of Medicine, University of Pennsylvania, Philadelphia, PA, 19104

#These authors contributed equally to this work

Keywords: lipid nanoparticles, protein adsorption, drug delivery, high-throughput screening, gene therapy

*Corresponding Author

Email: mjmitch@seas.upenn.edu

Table S1. Lipid nanoparticle (LNP) formulation parameters.

Lipid Nanoparticle	Molar Percentage of Component (%)				Mass Ratio
	Ionizable Lipid (C12-200)	Helper Lipid (DOPE or DSPC)	Lipid-PEG (PEG 1000, 2000, 3000, or 5000)	Cholesterol	Ionizable Lipid:b-DNA Ratio
1 (DOPE and PEG1000)	40	10	48.5	1.5	5:1
2 (DOPE and PEG1000)	40	10	48.5	1.5	10:1
3 (DOPE and PEG2000)	40	10	48.5	1.5	5:1
4 (DOPE and PEG2000)	40	10	48.5	1.5	10:1
5 (DOPE and PEG3000)	40	10	48.5	1.5	5:1
6 (DOPE and PEG3000)	40	10	48.5	1.5	10:1
7 (DOPE and PEG5000)	40	10	48.5	1.5	5:1
8 (DOPE and PEG5000)	40	10	48.5	1.5	10:1
9 (DOPE and PEG1000)	40	10	40	10	5:1
10 (DOPE and PEG1000)	40	10	40	10	10:1
11 (DOPE and PEG2000)	40	10	40	10	5:1
12 (DOPE and PEG2000)	40	10	40	10	10:1
13 (DOPE and PEG3000)	40	10	40	10	5:1
14 (DOPE and PEG3000)	40	10	40	10	10:1
15 (DOPE and PEG5000)	40	10	40	10	5:1
16 (DOPE and PEG5000)	40	10	40	10	10:1
17 (DOPE and PEG1000)	40	10	30	20	5:1
18 (DOPE and PEG1000)	40	10	30	20	10:1
19 (DOPE and PEG2000)	40	10	30	20	5:1
20 (DOPE and PEG2000)	40	10	30	20	10:1
21 (DOPE and PEG3000)	40	10	30	20	5:1
22 (DOPE and PEG3000)	40	10	30	20	10:1
23 (DOPE and PEG5000)	40	10	30	20	5:1
24 (DOPE and PEG5000)	40	10	30	20	10:1
25 (DOPE and PEG1000)	40	10	20	30	5:1
26 (DOPE and PEG1000)	40	10	20	30	10:1
27 (DOPE and PEG2000)	40	10	20	30	5:1
28 (DOPE and PEG2000)	40	10	20	30	10:1
29 (DOPE and PEG3000)	40	10	20	30	5:1
30 (DOPE and PEG3000)	40	10	20	30	10:1
31 (DOPE and PEG5000)	40	10	20	30	5:1
32 (DOPE and PEG5000)	40	10	20	30	10:1
33 (DOPE and PEG1000)	40	10	10	40	5:1
34 (DOPE and PEG1000)	40	10	10	40	10:1
35 (DOPE and PEG2000)	40	10	10	40	5:1
36 (DOPE and PEG2000)	40	10	10	40	10:1
37 (DOPE and PEG3000)	40	10	10	40	5:1
38 (DOPE and PEG3000)	40	10	10	40	10:1

39 (DOPE and PEG5000)	40	10	10	40	5:1
40 (DOPE and PEG5000)	40	10	10	40	10:1
41 (DOPE and PEG1000)	40	10	1.5	48.5	5:1
42 (DOPE and PEG1000)	40	10	1.5	48.5	10:1
43 (DOPE and PEG2000)	40	10	1.5	48.5	5:1
44 (DOPE and PEG2000)	40	10	1.5	48.5	10:1
45 (DOPE and PEG3000)	40	10	1.5	48.5	5:1
46 (DOPE and PEG3000)	40	10	1.5	48.5	10:1
47 (DOPE and PEG5000)	40	10	1.5	48.5	5:1
48 (DOPE and PEG5000)	40	10	1.5	48.5	10:1
49 (DSPC and PEG1000)	40	10	48.5	1.5	5:1
50 (DSPC and PEG1000)	40	10	48.5	1.5	10:1
51 (DSPC and PEG2000)	40	10	48.5	1.5	5:1
52 (DSPC and PEG2000)	40	10	48.5	1.5	10:1
53 (DSPC and PEG3000)	40	10	48.5	1.5	5:1
54 (DSPC and PEG3000)	40	10	48.5	1.5	10:1
55 (DSPC and PEG5000)	40	10	48.5	1.5	5:1
56 (DSPC and PEG5000)	40	10	48.5	1.5	10:1
57 (DSPC and PEG1000)	40	10	40	10	5:1
58 (DSPC and PEG1000)	40	10	40	10	10:1
59 (DSPC and PEG2000)	40	10	40	10	5:1
60 (DSPC and PEG2000)	40	10	40	10	10:1
61 (DSPC and PEG3000)	40	10	40	10	5:1
62 (DSPC and PEG3000)	40	10	40	10	10:1
63 (DSPC and PEG5000)	40	10	40	10	5:1
64 (DSPC and PEG5000)	40	10	40	10	10:1
65 (DSPC and PEG1000)	40	10	30	20	5:1
66 (DSPC and PEG1000)	40	10	30	20	10:1
67 (DSPC and PEG2000)	40	10	30	20	5:1
68 (DSPC and PEG2000)	40	10	30	20	10:1
69 (DSPC and PEG3000)	40	10	30	20	5:1
70 (DSPC and PEG3000)	40	10	30	20	10:1
71 (DSPC and PEG5000)	40	10	30	20	5:1
72 (DSPC and PEG5000)	40	10	30	20	10:1
73 (DSPC and PEG1000)	40	10	20	30	5:1
74 (DSPC and PEG1000)	40	10	20	30	10:1
75 (DSPC and PEG2000)	40	10	20	30	5:1
76 (DSPC and PEG2000)	40	10	20	30	10:1
77 (DSPC and PEG3000)	40	10	20	30	5:1
78 (DSPC and PEG3000)	40	10	20	30	10:1
79 (DSPC and PEG5000)	40	10	20	30	5:1
80 (DSPC and PEG5000)	40	10	20	30	10:1
81 (DSPC and PEG1000)	40	10	10	40	5:1
82 (DSPC and PEG1000)	40	10	10	40	10:1
83 (DSPC and PEG2000)	40	10	10	40	5:1
84 (DSPC and PEG2000)	40	10	10	40	10:1

85 (DSPC and PEG3000)	40	10	10	40	5:1
86 (DSPC and PEG3000)	40	10	10	40	10:1
87 (DSPC and PEG5000)	40	10	10	40	5:1
88 (DSPC and PEG5000)	40	10	10	40	10:1
89 (DSPC and PEG1000)	40	10	1.5	48.5	5:1
90 (DSPC and PEG1000)	40	10	1.5	48.5	10:1
91 (DSPC and PEG2000)	40	10	1.5	48.5	5:1
92 (DSPC and PEG2000)	40	10	1.5	48.5	10:1
93 (DSPC and PEG3000)	40	10	1.5	48.5	5:1
94 (DSPC and PEG3000)	40	10	1.5	48.5	10:1
95 (DSPC and PEG5000)	40	10	1.5	48.5	5:1
96 (DSPC and PEG5000)	40	10	1.5	48.5	10:1
Naked Barcode	0	0	0	0	0

Table S2. LNPs were characterized for size and polydispersity (PDI) by dynamic light scattering (DLS). LNPs denoted N/A were excluded from the injected pool based on analysis of DLS peaks and autocorrelation data.

Lipid Nanoparticle	Z-Ave (d.nm)	PDI
1	64.91	0.177
2	91.96	0.148
3	109.9	0.163
4	114.2	0.181
5	135.8	0.071
6	140.1	0.077
7	124.1	0.189
8	128.2	0.019
9	107	0.172
10	118.6	0.017
11	148.9	0.045
12	130.5	0.161
13	152.2	0.052
14	146.9	0.08
15	144.1	0.011
16	129.3	0.165
17	131.6	0.186
18	108.8	0.185
19	139.4	0.118
20	139	0.146
21	152.9	0.078
22	154.4	0.029
23	130.2	0.095
24	131.7	0.006
25	130.3	0.129
26	121.7	0.141
27	153.9	0.002
28	148	0.023
29	154.7	0.106
30	154.5	0.09
31	153.3	0.085
32	146.3	0.019
33	144.4	0.13
34	138	0.094
35	150.6	0.073
36	155.6	0.114
37	163.9	0.115
38	160.9	0.085
39	150.1	0.038
40	159	0.03
41	180.6	0.145

42	170.5	0.074
43	162.8	0.043
44	166.1	0.094
45	170.7	0.063
46	166.1	0.111
47	171.4	0.061
48	173	0.104
49	N/A	N/A
50	88.87	0.106
51	90.47	0.261
52	91.93	0.19
53	117.7	0.016
54	128.5	0.035
55	115.1	0.079
56	N/A	N/A
57	94.74	0.191
58	122.8	0.013
59	118.6	0.043
60	125.4	0.03
61	120	0.093
62	148.4	0.037
63	123.1	0.059
64	118.6	0.114
65	107.9	0.208
66	73.25	0.216
67	131	0.039
68	126.8	0.067
69	138.9	0.104
70	134	0.078
71	122.5	0.077
72	132.8	0.007
73	120.9	0.153
74	111.6	0.13
75	132.2	0.118
76	134.9	0.097
77	144.6	0.064
78	136	0.074
79	143.6	0.103
80	148.2	0.042
81	141.3	0.103
82	124.2	0.087
83	134.8	0.116
84	131.4	0.113
85	154.9	0.076
86	157.8	0.091
87	156.1	0.061

88	154.2	0.087
89	173.2	0.098
90	167.2	0.111
91	165.9	0.106
92	164.5	0.069
93	172	0.096
94	168.3	0.105
95	162.9	0.093
96	158.4	0.08

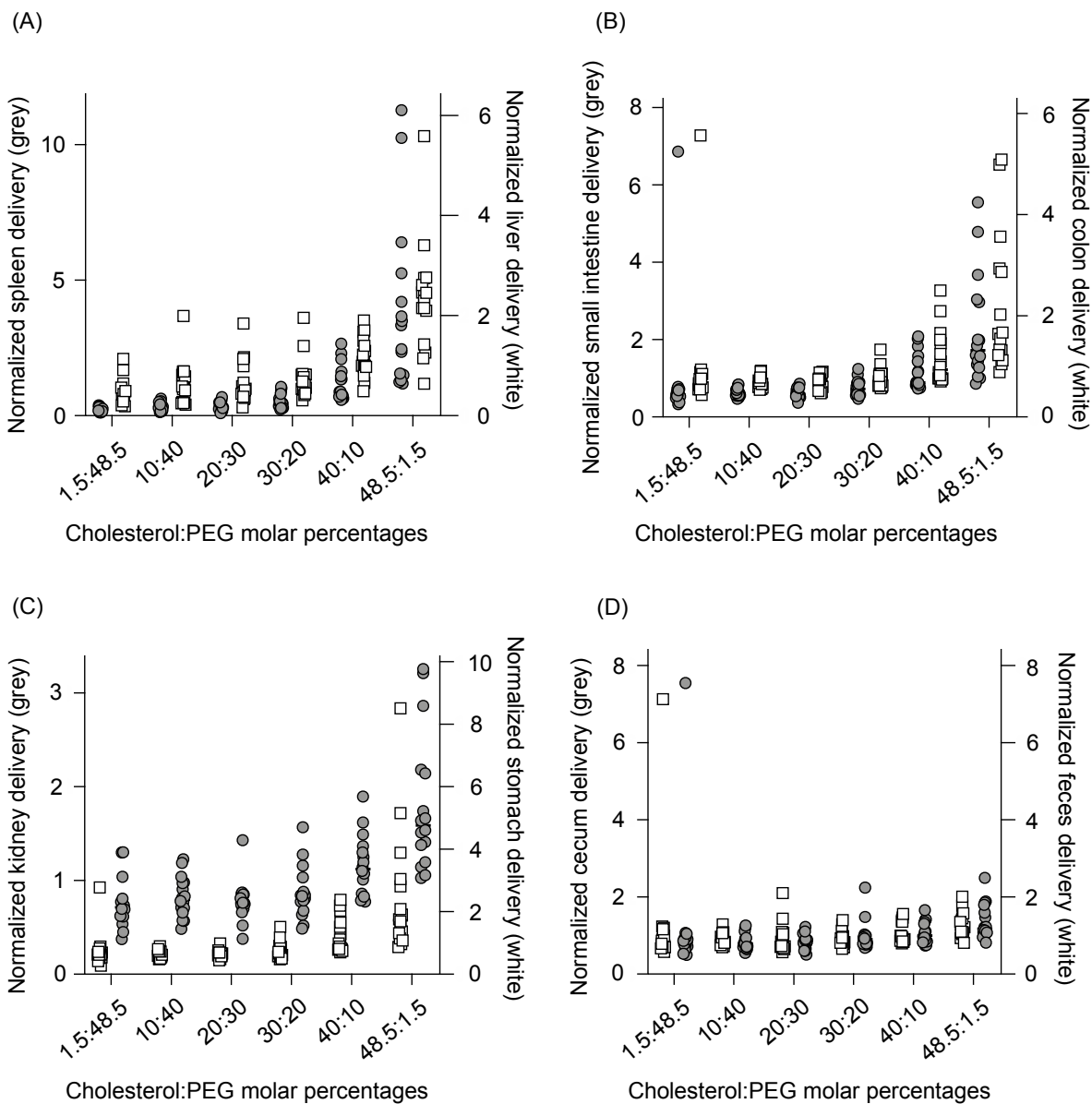


Figure S1. LNPs formulated with higher ratios of cholesterol to lipid-PEG accumulated to a higher degree in most tissues analyzed. LNPs were formulated with 1 ionizable lipid (C12-200), 6 different excipient molar ratios, 2 different ionizable lipid:b-DNA weight ratios, 2 different helper lipids, and 4 different lipid-anchored polyethylene glycol (PEG) conjugates. Details on specific excipient molar ratios for each LNP are provided in **Table S1**. 94 out of 96 formulations formed stable LNPs based on DLS data. LNP formulations were pooled together and injected to C57BL/6 mice via tail vein (N=4). Tissues were isolated six hours post injection and accumulation of b-DNA was quantified by deep sequencing. LNP accumulation in the (A) spleen and liver, (B) small intestine and colon, (C) kidney and stomach, and (D) cecum and feces was plotted based on the molar ratio of cholesterol to lipid-PEG.

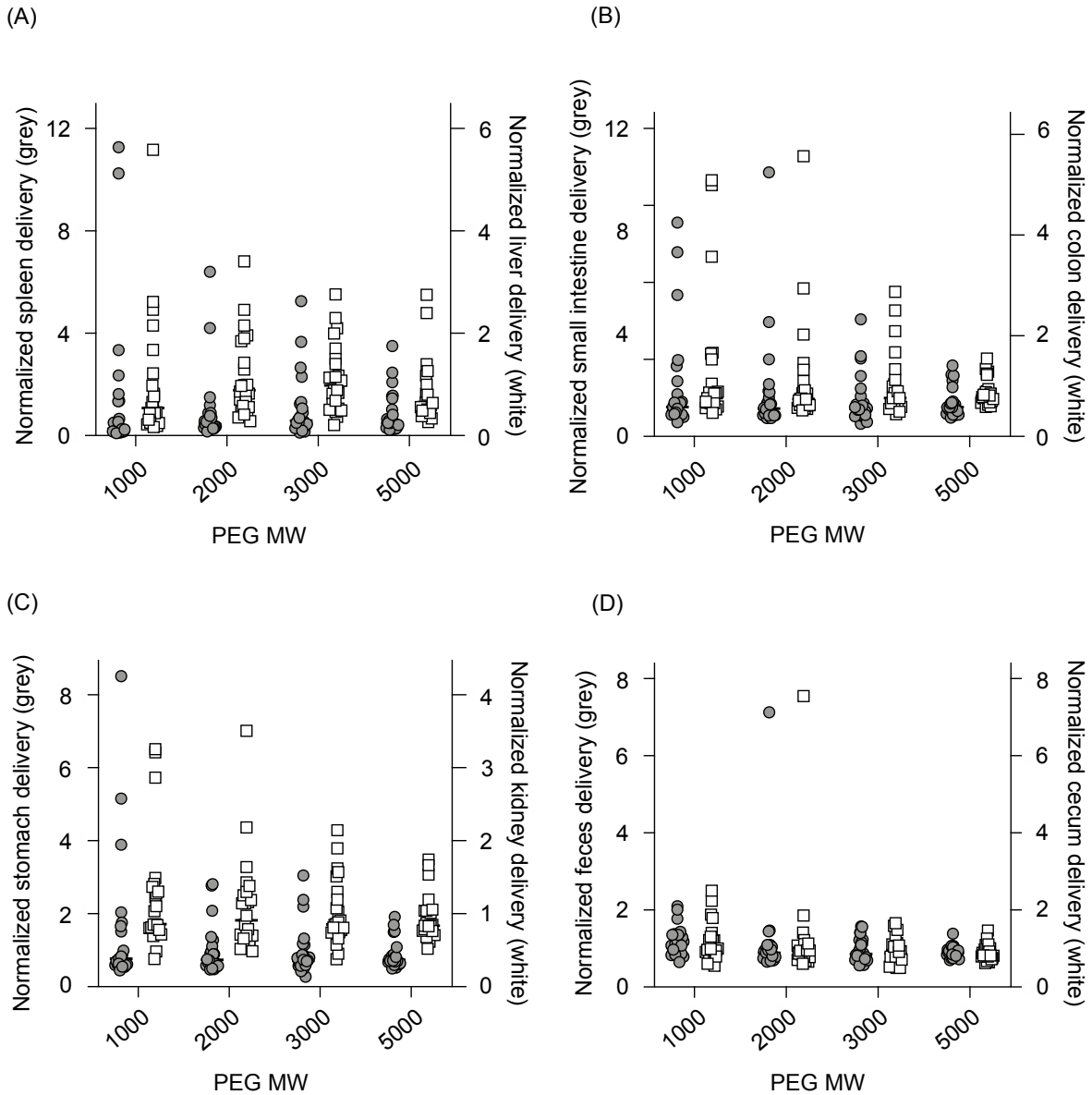


Figure S2. LNPs formulated with lower molecular lipid-PEGs accumulated to a higher degree in most tissues analyzed. LNPs were formulated with 1 ionizable lipid (C12-200), 6 different excipient molar ratios, 2 different ionizable lipid:b-DNA weight ratios, 2 different helper lipids, and 4 different lipid-anchored polyethylene glycol (PEG) conjugates. Details on specific excipient molar ratios for each LNP are provided in **Table S1**. 94 out of 96 formulations formed stable LNPs based on DLS data. LNP formulations were pooled together and injected to C57BL/6 mice via tail vein (N=4). Tissues were isolated six hours post injection and accumulation of b-DNA was quantified by deep sequencing. LNP accumulation in the (A) spleen and liver, (B) small intestine and colon, (C) stomach and kidney, and (D) feces and cecum was plotted based on the molecular weight of the lipid-PEG incorporated into the LNPs.

Supplementary Discussion of QCM-D Experiments

Figure 4B in the main text presented the frequency shift of the third overtone ($\Delta F_3/3$) versus time for LNPs formulated with the C12-200 ionizable lipid^[1]. The time dependency has been removed in **Figure S3A** by plotting the measured dissipation ΔD_n against $\Delta F_n/n$, where n is the overtone. Plots of ΔD_n vs $\Delta F_n/n$ allow kinetic processes (e.g. adsorption or conformational changes) to be compared^[2]. Data between values of $\Delta F_n/n$ between 0 and ~ -60 Hz correspond to the adsorption of ApoE on the Au coated sensor. The curves begin to diverge at larger negative frequency shifts as particle adsorption takes place. Here, for a given frequency shift the LNP formulated with DOPE (LNP 42) have a lower dissipation value than the LNP formulated with DSPC (LNP 90) for the same overtone. Control experiments for LNPs formulated with C12-200 interacting with a bare Au sensor show the opposite trend with a larger negative frequency shift for the DSPC formulation (**Figure S4**), which is the reverse of the magnitudes observed in the presence of ApoE and is further evidence of specific interactions between the DOPE-containing LNPs and ApoE. Dissipation from heterogenous films of discrete, adsorbed particles arises from both hydrodynamic interactions with the particles and deformation of particle-surface contacts, with the majority of energy dissipated through the liquid.^[3,4] One possible interpretation of the lower dissipation, is that ApoE forms wider, more rigid contacts with the DOPE-containing LNPs compared to DSPC-containing LNPs. However, the presence of the homogeneous, viscoelastic ApoE layer complicates the interpretation, and finite element methods are required for quantitative analysis^[4]. Regardless, **Figure S3A** clearly demonstrates the nature of the adsorption depends on the choice of helper lipid.

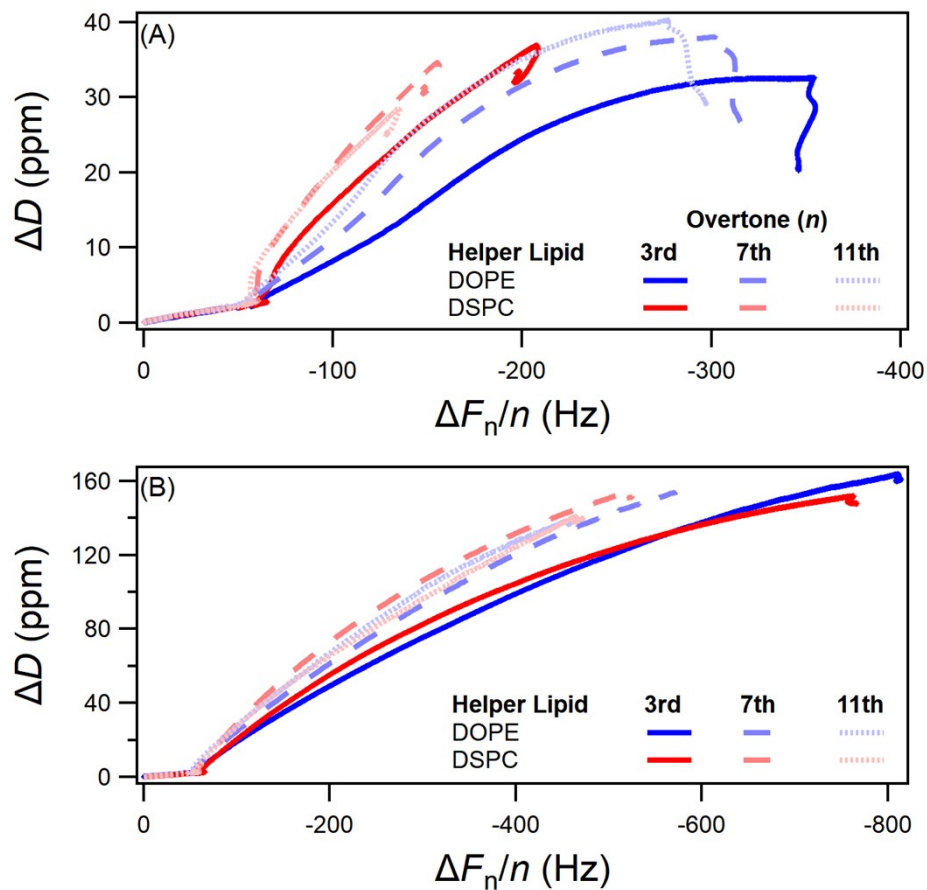


Fig S3. Kinetic pathways of LNP adsorption. (A) Dissipation values vs frequency shift ($\Delta F_n/n$) follow different adsorption pathways at each overtone depending on choice of helper lipid for particles containing C12-200 (DOPE = LNP 42, DSPC = LNP 90). (B) Adsorption pathways are similar when C14-4 ionizable lipids are used. Note that the composition of the C14-4 containing LNPs is otherwise identical to the equivalent C12-200 LNPs.

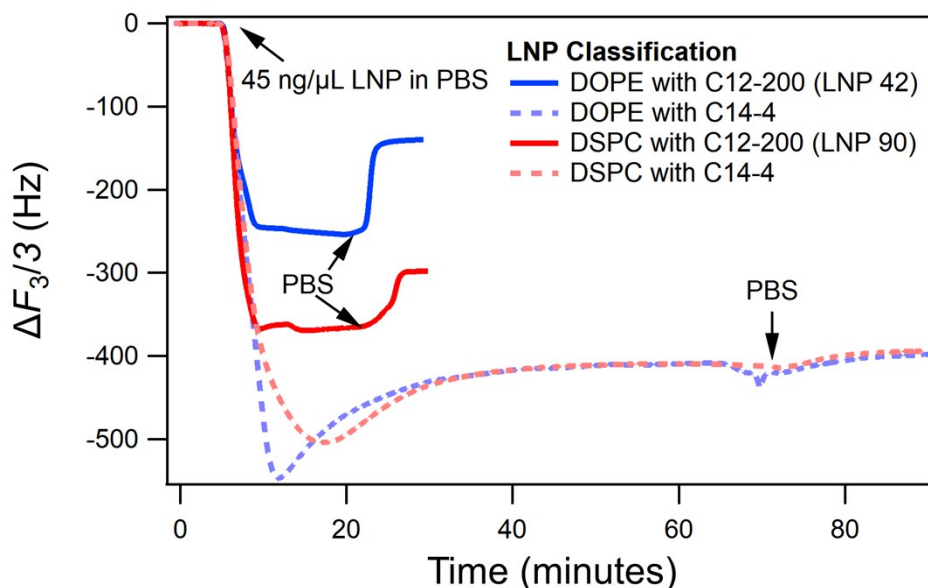


Fig S4. Change in frequency of the third overtone versus time for LNPs adsorbing onto Au-coated QCM-D crystals. LNPs vary by identity of the helper lipid (DOPE or DSPC) and the ionizable lipid (C12-200 or C14-4), but otherwise had identical compositions.

In contrast to the data in **Figure S3A**, control experiments for LNPs formulated with the C14-4 ionizable lipid^[5] displayed no significant difference in the nature of their adsorption (**Figure S3B**). However, **Figure S5** demonstrates that the nature of the helper lipid has a strong influence on the initial rate of adsorption of these control particles. In particular, **Figure S5B** shows that the peak rate of change of the frequency shift of the 3rd overtone was approximately 3 times larger for the DOPE containing formulation than the DSPC containing formulation. Control experiments that looked at adsorption of these particles on bare Au sensors showed no significant difference in the rate of initial particle adsorption (**Figure S4**). This suggests that adsorption is aided by specific interactions between DOPE and ApoE.

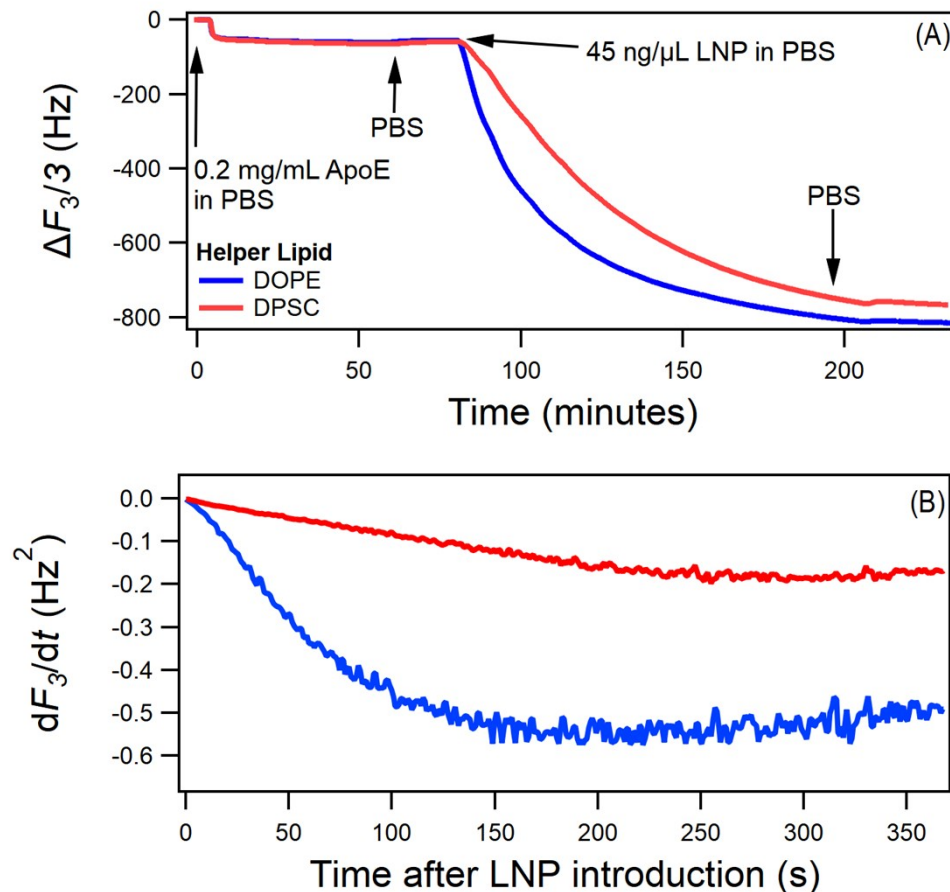
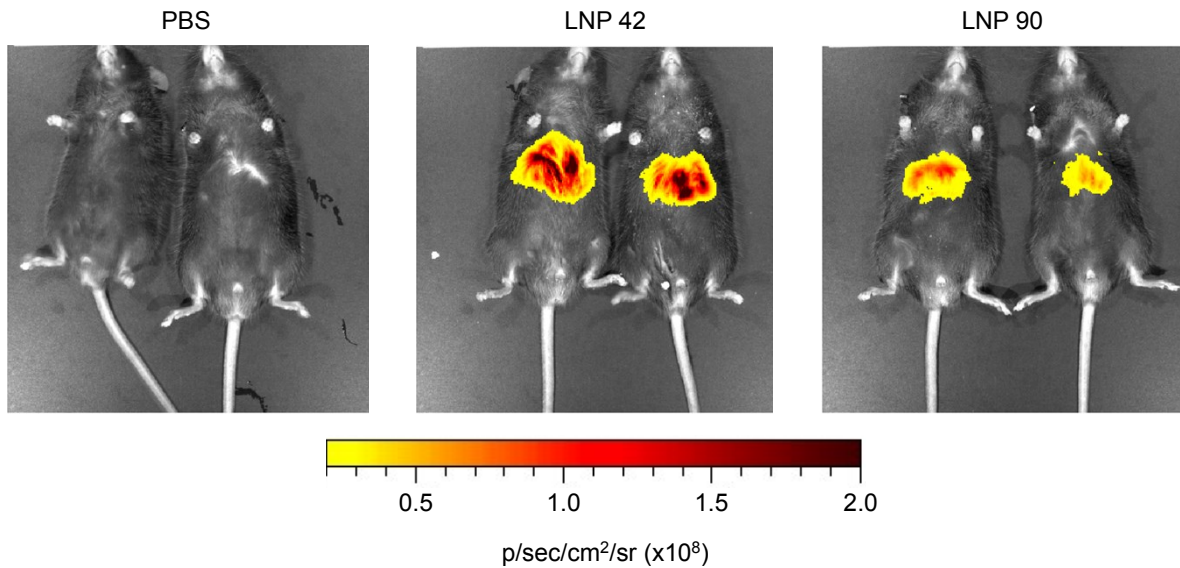


Fig S5. (A) Change in frequency of the third overtone versus time for LNPs containing C14-4 ionizable lipid adsorbing onto ApoE-coated QCM-D crystals. Aside from the ionizable lipids, the composition of these LNPs is identical to the equivalent DOPE (LNP 42) and DSPC (LNP 90) containing particles. (B) Rate of change of frequency relative to time after the introduction of the LNPs.

Further control experiments were performed investigating LNP interactions with bare Au sensors. Measured frequency shifts of the third overtone are shown in **Figure S4**. Here, all formulations showed strong interactions with the Au surface and are stable to rinsing with PBS. LNPs formulated with the ionizable lipid C14-4 resulted in a larger frequency shift when compared to the C12-200 LNPs, which may result from stronger adsorption and/or larger LNPs. For the C14-4 containing LNPs, a peak in the frequency is also observed during adsorption. This peak may result from rupture and/or fusion of the nanoparticles, as often seen for phospholipid assemblies adsorbing on solid supports.^[6] However, the large magnitude of the plateau frequency shifts suggests that the LNPs did not rupture completely, if at all. It is possible that stronger interactions with the underlying Au substrate and/or that hydrodynamic contributions from the larger LNP size mask the contribution of ApoE-LNP contact results in the similar nature of adsorption on ApoE observed in **Figure S3B**.

Additional Supplementary Information

(A)



(B)

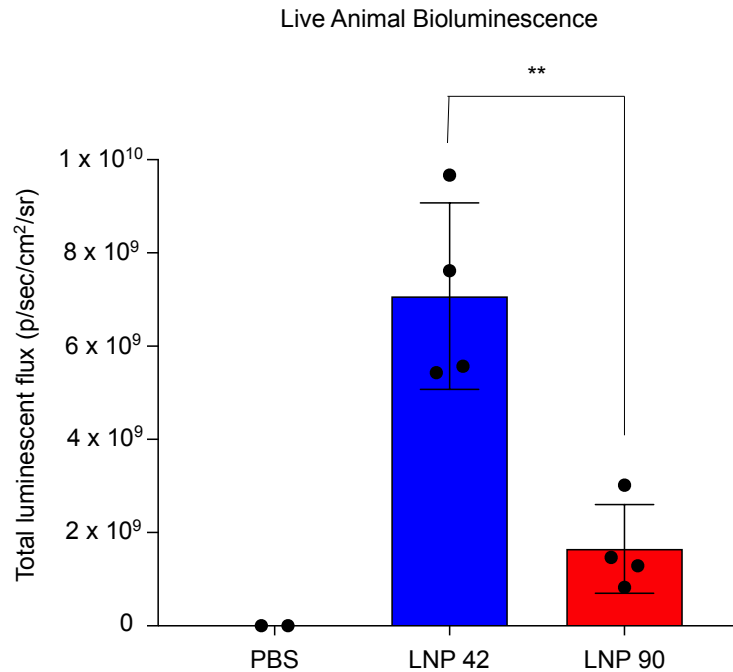


Fig S6. Firefly luciferase mRNA-LNPs were administered via tail vein injection. LNP 42 and LNP 90 were formulated by microfluidic mixing to encapsulate mRNA encoding for firefly luciferase. C57BL/6 mice were intravenously injected with either LNP 42 or LNP 90 at 0.2 mg/kg mRNA via tail vein. Total luminescent flux was quantified 6 hours post-injection (**P=0.0027). N=4 mice per experimental group. N=2 mice per PBS control group. Representative images for N=2 mice are shown. Data was plotted as mean \pm SD. **P<0.005 by t-test.

Table S3. Library of b-DNA sequences. NNNNNNNNNN represents unique molecular identifiers (UMI). *denotes phosphorothioate bond locations.

Barcode	b-DNA Sequence
b-DNA 1	A*G*A* C*G*TGTGCTCTCCGATCTGAGGGTACTTNNNNNNNNNN AGATCGGAAGAGCGT*C*G *T*G*T
b-DNA 2	A*G*A* C*G*TGTGCTCTCCGATCTGACAATTGCCNNNNNNNNNN AGATCGGAAGAGCGT*C*G *T*G*T
b-DNA 3	A*G*A* C*G*TGTGCTCTCCGATCTTAACGCACCTNNNNNNNNNN AGATCGGAAGAGCGT*C*G *T*G*T
b-DNA 4	A*G*A* C*G*TGTGCTCTCCGATCTATGATCGTCGNNNNNNNNNN AGATCGGAAGAGCGT*C*G *T*G*T
b-DNA 5	A*G*A* C*G*TGTGCTCTCCGATCTTGTCTCCATNNNNNNNNNN AGATCGGAAGAGCGT*C*G *T*G*T
b-DNA 6	A*G*A* C*G*TGTGCTCTCCGATCTGGAGAAACAGNNNNNNNNNN AGATCGGAAGAGCGT*C*G *T*G*T
b-DNA 7	A*G*A* C*G*TGTGCTCTCCGATCTCGTACAAACGNNNNNNNNNN AGATCGGAAGAGCGT*C*G *T*G*T
b-DNA 8	A*G*A* C*G*TGTGCTCTCCGATCTGATTTGTGGNNNNNNNNNN AGATCGGAAGAGCGT*C*G *T*G*T
b-DNA 9	A*G*A* C*G*TGTGCTCTCCGATCTTTCAGCCTTNNNNNNNNNN AGATCGGAAGAGCGT*C*G *T*G*T
b-DNA 10	A*G*A* C*G*TGTGCTCTCCGATCTGAATGCTGACNNNNNNNNNN AGATCGGAAGAGCGT*C*G *T*G*T
b-DNA 11	A*G*A* C*G*TGTGCTCTCCGATCTATCCATGAGGNNNNNNNNNN AGATCGGAAGAGCGT*C*G *T*G*T
b-DNA 12	A*G*A* C*G*TGTGCTCTCCGATCTTCCACGATGNNNNNNNNNN AGATCGGAAGAGCGT*C*G *T*G*T
b-DNA 13	A*G*A* C*G*TGTGCTCTCCGATCTGCTGGGAATTNNNNNNNNNN AGATCGGAAGAGCGT*C*G *T*G*T
b-DNA 14	A*G*A* C*G*TGTGCTCTCCGATCTCAAACGACGNNNNNNNNNN AGATCGGAAGAGCGT*C*G *T*G*T
b-DNA 15	A*G*A* C*G*TGTGCTCTCCGATCTTCTCGCCTTNNNNNNNNNN AGATCGGAAGAGCGT*C*G *T*G*T
b-DNA 16	A*G*A* C*G*TGTGCTCTCCGATCTCAGATCAGAGNNNNNNNNNN AGATCGGAAGAGCGT*C*G *T*G*T
b-DNA 17	A*G*A* C*G*TGTGCTCTCCGATCTGACACGTTCTNNNNNNNNNN AGATCGGAAGAGCGT*C*G *T*G*T
b-DNA 18	A*G*A* C*G*TGTGCTCTCCGATCTGCTAAGTCTNNNNNNNNNN AGATCGGAAGAGCGT*C*G *T*G*T
b-DNA 19	A*G*A* C*G*TGTGCTCTCCGATCTTGTTCGACCTNNNNNNNNNN AGATCGGAAGAGCGT*C*G *T*G*T
b-DNA 20	A*G*A* C*G*TGTGCTCTCCGATCTCCCAAAGACANNNNNNNNNN AGATCGGAAGAGCGT*C*G *T*G*T
b-DNA 21	A*G*A* C*G*TGTGCTCTCCGATCTCAGGTAGGAANNNNNNNNNN AGATCGGAAGAGCGT*C*G *T*G*T
b-DNA 22	A*G*A* C*G*TGTGCTCTCCGATCTCATTATCGCGNNNNNNNNNN AGATCGGAAGAGCGT*C*G *T*G*T
b-DNA 23	A*G*A* C*G*TGTGCTCTCCGATCTCAGAGACTGANNNNNNNNNN AGATCGGAAGAGCGT*C*G *T*G*T
b-DNA 24	A*G*A* C*G*TGTGCTCTCCGATCTTGACATGCACNNNNNNNNNN AGATCGGAAGAGCGT*C*G *T*G*T
b-DNA 25	A*G*A* C*G*TGTGCTCTCCGATCTTGTGTTCCNNNNNNNNNN AGATCGGAAGAGCGT*C*G *T*G*T
b-DNA 26	A*G*A* C*G*TGTGCTCTCCGATCTCTCTGAACNNNNNNNNNN AGATCGGAAGAGCGT*C*G *T*G*T
b-DNA 27	A*G*A* C*G*TGTGCTCTCCGATCTACTAGCCANNNNNNNNNN AGATCGGAAGAGCGT*C*G *T*G*T
b-DNA 28	A*G*A* C*G*TGTGCTCTCCGATCTTGACTTTGCCNNNNNNNNNN AGATCGGAAGAGCGT*C*G *T*G*T
b-DNA 29	A*G*A* C*G*TGTGCTCTCCGATCTTTCAGCGAAGNNNNNNNNNN AGATCGGAAGAGCGT*C*G *T*G*T
b-DNA 30	A*G*A* C*G*TGTGCTCTCCGATCTACAGGCATACNNNNNNNNNN AGATCGGAAGAGCGT*C*G *T*G*T
b-DNA 31	A*G*A* C*G*TGTGCTCTCCGATCTCGACTCCTAANNNNNNNNNN AGATCGGAAGAGCGT*C*G *T*G*T
b-DNA 32	A*G*A* C*G*TGTGCTCTCCGATCTCACGCTATCTNNNNNNNNNN AGATCGGAAGAGCGT*C*G *T*G*T
b-DNA 33	A*G*A* C*G*TGTGCTCTCCGATCTAAGTCCGCTTNNNNNNNNNN AGATCGGAAGAGCGT*C*G *T*G*T
b-DNA 34	A*G*A* C*G*TGTGCTCTCCGATCTATCTAGACGNNNNNNNNNN AGATCGGAAGAGCGT*C*G *T*G*T
b-DNA 35	A*G*A* C*G*TGTGCTCTCCGATCTAATCCCCCTTNNNNNNNNNN AGATCGGAAGAGCGT*C*G *T*G*T
b-DNA 36	A*G*A* C*G*TGTGCTCTCCGATCTTTCGCATCTGNNNNNNNNNN AGATCGGAAGAGCGT*C*G *T*G*T
b-DNA 37	A*G*A* C*G*TGTGCTCTCCGATCTTGGAGTTCNNNNNNNNNN AGATCGGAAGAGCGT*C*G *T*G*T

b-DNA 38	A*G*A* C*G*TGTGCTCTCCGATCTTTGGCCAATCNNNNNNNNNN AGATCGGAAGAGCGT*C*G *T*G*T
b-DNA 39	A*G*A* C*G*TGTGCTCTCCGATCTAAAGGCGACANNNNNNNNNN AGATCGGAAGAGCGT*C*G *T*G*T
b-DNA 40	A*G*A* C*G*TGTGCTCTCCGATCTAATGTCGCTGNNNNNNNNNN AGATCGGAAGAGCGT*C*G *T*G*T
b-DNA 41	A*G*A* C*G*TGTGCTCTCCGATCTCAACGTATGGNNNNNNNNNN AGATCGGAAGAGCGT*C*G *T*G*T
b-DNA 42	A*G*A* C*G*TGTGCTCTCCGATCTCTACCTAACNNNNNNNNNN AGATCGGAAGAGCGT*C*G *T*G*T
b-DNA 43	A*G*A* C*G*TGTGCTCTCCGATCTTCACGGTGTANNNNNNNNNN AGATCGGAAGAGCGT*C*G *T*G*T
b-DNA 44	A*G*A* C*G*TGTGCTCTCCGATCTCCCAGAAGTANNNNNNNNNN AGATCGGAAGAGCGT*C*G *T*G*T
b-DNA 45	A*G*A* C*G*TGTGCTCTCCGATCTACAAGCGTTNNNNNNNNNN AGATCGGAAGAGCGT*C*G *T*G*T
b-DNA 46	A*G*A* C*G*TGTGCTCTCCGATCTGGATTAACCGNNNNNNNNNN AGATCGGAAGAGCGT*C*G *T*G*T
b-DNA 47	A*G*A* C*G*TGTGCTCTCCGATCTCCTCGTGATANNNNNNNNNN AGATCGGAAGAGCGT*C*G *T*G*T
b-DNA 48	A*G*A* C*G*TGTGCTCTCCGATCTGACTATTCGGNNNNNNNNNN AGATCGGAAGAGCGT*C*G *T*G*T
b-DNA 49	A*G*A* C*G*TGTGCTCTCCGATCTATCGTCTCAANNNNNNNNNN AGATCGGAAGAGCGT*C*G *T*G*T
b-DNA 50	A*G*A* C*G*TGTGCTCTCCGATCTGCGTTATGACNNNNNNNNNN AGATCGGAAGAGCGT*C*G *T*G*T
b-DNA 51	A*G*A* C*G*TGTGCTCTCCGATCTGTTTACGTGTNNNNNNNNNN AGATCGGAAGAGCGT*C*G *T*G*T
b-DNA 52	A*G*A* C*G*TGTGCTCTCCGATCTGTACAATGGCNNNNNNNNNN AGATCGGAAGAGCGT*C*G *T*G*T
b-DNA 53	A*G*A* C*G*TGTGCTCTCCGATCTCTAGGCGGATNNNNNNNNNN AGATCGGAAGAGCGT*C*G *T*G*T
b-DNA 54	A*G*A* C*G*TGTGCTCTCCGATCTCATTGGTTGANNNNNNNNNN AGATCGGAAGAGCGT*C*G *T*G*T
b-DNA 55	A*G*A* C*G*TGTGCTCTCCGATCTCAGAAGTGGCNNNNNNNNNN AGATCGGAAGAGCGT*C*G *T*G*T
b-DNA 56	A*G*A* C*G*TGTGCTCTCCGATCTCAGGAACACCNNNNNNNNNN AGATCGGAAGAGCGT*C*G *T*G*T
b-DNA 57	A*G*A* C*G*TGTGCTCTCCGATCTTTCGTGACCTNNNNNNNNNN AGATCGGAAGAGCGT*C*G *T*G*T
b-DNA 58	A*G*A* C*G*TGTGCTCTCCGATCTTCGGAAAGANNNNNNNNNN AGATCGGAAGAGCGT*C*G *T*G*T
b-DNA 59	A*G*A* C*G*TGTGCTCTCCGATCTAGTGTGAGAGNNNNNNNNNN AGATCGGAAGAGCGT*C*G *T*G*T
b-DNA 60	A*G*A* C*G*TGTGCTCTCCGATCTCTGAACACATNNNNNNNNNN AGATCGGAAGAGCGT*C*G *T*G*T
b-DNA 61	A*G*A* C*G*TGTGCTCTCCGATCTAGGGTGTAAANNNNNNNNNN AGATCGGAAGAGCGT*C*G *T*G*T
b-DNA 62	A*G*A* C*G*TGTGCTCTCCGATCTTGGGGTTAGNNNNNNNNNN AGATCGGAAGAGCGT*C*G *T*G*T
b-DNA 63	A*G*A* C*G*TGTGCTCTCCGATCTGGCAACGTACNNNNNNNNNN AGATCGGAAGAGCGT*C*G *T*G*T
b-DNA 64	A*G*A* C*G*TGTGCTCTCCGATCTCACTATAGGCNNNNNNNNNN AGATCGGAAGAGCGT*C*G *T*G*T
b-DNA 65	A*G*A* C*G*TGTGCTCTCCGATCTTTCACCAGCCNNNNNNNNNN AGATCGGAAGAGCGT*C*G *T*G*T
b-DNA 66	A*G*A* C*G*TGTGCTCTCCGATCTAATCGGTGAANNNNNNNNNN AGATCGGAAGAGCGT*C*G *T*G*T
b-DNA 67	A*G*A* C*G*TGTGCTCTCCGATCTTCTATGCACTNNNNNNNNNN AGATCGGAAGAGCGT*C*G *T*G*T
b-DNA 68	A*G*A* C*G*TGTGCTCTCCGATCTGAGAACGGTNNNNNNNNNN AGATCGGAAGAGCGT*C*G *T*G*T
b-DNA 69	A*G*A* C*G*TGTGCTCTCCGATCTTATGTGTACGNNNNNNNNNN AGATCGGAAGAGCGT*C*G *T*G*T
b-DNA 70	A*G*A* C*G*TGTGCTCTCCGATCTCTCTCTTGCANNNNNNNNNN AGATCGGAAGAGCGT*C*G *T*G*T
b-DNA 71	A*G*A* C*G*TGTGCTCTCCGATCTTCGCAACGAGNNNNNNNNNN AGATCGGAAGAGCGT*C*G *T*G*T
b-DNA 72	A*G*A* C*G*TGTGCTCTCCGATCTGGTGAGCAATNNNNNNNNNN AGATCGGAAGAGCGT*C*G *T*G*T
b-DNA 73	A*G*A* C*G*TGTGCTCTCCGATCTTTCATTGCGCNNNNNNNNNN AGATCGGAAGAGCGT*C*G *T*G*T
b-DNA 74	A*G*A* C*G*TGTGCTCTCCGATCTTGATGCTTGANNNNNNNNNN AGATCGGAAGAGCGT*C*G *T*G*T
b-DNA 75	A*G*A* C*G*TGTGCTCTCCGATCTTAACGCCAAGNNNNNNNNNN AGATCGGAAGAGCGT*C*G *T*G*T
b-DNA 76	A*G*A* C*G*TGTGCTCTCCGATCTGGGTTGCGATNNNNNNNNNN AGATCGGAAGAGCGT*C*G *T*G*T
b-DNA 77	A*G*A* C*G*TGTGCTCTCCGATCTGAGACAACCGNNNNNNNNNN AGATCGGAAGAGCGT*C*G *T*G*T
b-DNA 78	A*G*A* C*G*TGTGCTCTCCGATCTGGATGACCTCNNNNNNNNNN AGATCGGAAGAGCGT*C*G *T*G*T
b-DNA 79	A*G*A* C*G*TGTGCTCTCCGATCTGTGGCATGTTNNNNNNNNNN AGATCGGAAGAGCGT*C*G *T*G*T
b-DNA 80	A*G*A* C*G*TGTGCTCTCCGATCTAAGGATGTGGNNNNNNNNNN AGATCGGAAGAGCGT*C*G *T*G*T

b-DNA 81	A*G*A* C*G*TGTGCTCTCCGATCTTCGAGACANNNNNNNNNN AGATCGGAAGAGCGT*C*G *T*G*T
b-DNA 82	A*G*A* C*G*TGTGCTCTCCGATCTAAGTCTCCGNNNNNNNNNN AGATCGGAAGAGCGT*C*G *T*G*T
b-DNA 83	A*G*A* C*G*TGTGCTCTCCGATCTCAAGACTGCANNNNNNNNNN AGATCGGAAGAGCGT*C*G *T*G*T
b-DNA 84	A*G*A* C*G*TGTGCTCTCCGATCTGAGATTTCTNNNNNNNNNN AGATCGGAAGAGCGT*C*G *T*G*T
b-DNA 85	A*G*A* C*G*TGTGCTCTCCGATCTACTAGAAGGCNNNNNNNNNN AGATCGGAAGAGCGT*C*G *T*G*T
b-DNA 86	A*G*A* C*G*TGTGCTCTCCGATCTGCAATGGGAGNNNNNNNNNN AGATCGGAAGAGCGT*C*G *T*G*T
b-DNA 87	A*G*A* C*G*TGTGCTCTCCGATCTGACTCTCCAGNNNNNNNNNN AGATCGGAAGAGCGT*C*G *T*G*T
b-DNA 88	A*G*A* C*G*TGTGCTCTCCGATCTTGTGCTCGTANNNNNNNNNN AGATCGGAAGAGCGT*C*G *T*G*T
b-DNA 89	A*G*A* C*G*TGTGCTCTCCGATCTAGCATTATCCNNNNNNNNNN AGATCGGAAGAGCGT*C*G *T*G*T
b-DNA 90	A*G*A* C*G*TGTGCTCTCCGATCTGATTACCAACNNNNNNNNNN AGATCGGAAGAGCGT*C*G *T*G*T
b-DNA 91	A*G*A* C*G*TGTGCTCTCCGATCTGCCTTGATTGNNNNNNNNNN AGATCGGAAGAGCGT*C*G *T*G*T
b-DNA 92	A*G*A* C*G*TGTGCTCTCCGATCTGTCTCCATCNNNNNNNNNN AGATCGGAAGAGCGT*C*G *T*G*T
b-DNA 93	A*G*A* C*G*TGTGCTCTCCGATCTTACGCCACANNNNNNNNNN AGATCGGAAGAGCGT*C*G *T*G*T
b-DNA 94	A*G*A* C*G*TGTGCTCTCCGATCTGGAACGAGGTNNNNNNNNNN AGATCGGAAGAGCGT*C*G *T*G*T
b-DNA 95	A*G*A* C*G*TGTGCTCTCCGATCTCGGTGCAATCNNNNNNNNNN AGATCGGAAGAGCGT*C*G *T*G*T
b-DNA 96	A*G*A* C*G*TGTGCTCTCCGATCTAACCTTTGGGNNNNNNNNNN AGATCGGAAGAGCGT*C*G *T*G*T
b-DNA 97	A*G*A* C*G*TGTGCTCTCCGATCTGTAGAAGCTNNNNNNNNNN AGATCGGAAGAGCGT*C*G *T*G*T
b-DNA 98	A*G*A* C*G*TGTGCTCTCCGATCTCCCATCATGCNNNNNNNNNN AGATCGGAAGAGCGT*C*G *T*G*T
b-DNA 99	A*G*A* C*G*TGTGCTCTCCGATCTTGATGGCAANNNNNNNNNN AGATCGGAAGAGCGT*C*G *T*G*T
b-DNA 100	A*G*A* C*G*TGTGCTCTCCGATCTGCTCATGGAGNNNNNNNNNN AGATCGGAAGAGCGT*C*G *T*G*T

Table S4. Library of full-length reverse primers used in preparing the b-DNA library for deep sequencing.

Primers	Sequence
Miseq_primer 1	CAAGCAGAAGACGGCATAACGAGATCTGGTAGGTGACTGGAGTTCAGACGTGTG
Miseq_primer 2	CAAGCAGAAGACGGCATAACGAGATTAAGCATGGTACTGGAGTTCAGACGTGTG
Miseq_primer 3	CAAGCAGAAGACGGCATAACGAGATAGATGTGCGTGACTGGAGTTCAGACGTGTG
Miseq_primer 4	CAAGCAGAAGACGGCATAACGAGATGTCGAGCAGTACTGGAGTTCAGACGTGTG
Miseq_primer 5	CAAGCAGAAGACGGCATAACGAGATGAATTGCTGTGACTGGAGTTCAGACGTGTG
Miseq_primer 6	CAAGCAGAAGACGGCATAACGAGATAAGCAACTGTGACTGGAGTTCAGACGTGTG
Miseq_primer 7	CAAGCAGAAGACGGCATAACGAGATTAAGTAACTGGGTGACTGGAGTTCAGACGTGTG
Miseq_primer 8	CAAGCAGAAGACGGCATAACGAGATAGGCTCAAGTACTGGAGTTCAGACGTGTG
Miseq_primer 9	CAAGCAGAAGACGGCATAACGAGATCAGTTGGTGTGACTGGAGTTCAGACGTGTG
Miseq_primer 10	CAAGCAGAAGACGGCATAACGAGATTCTGGACCGTACTGGAGTTCAGACGTGTG
Miseq_primer 11	CAAGCAGAAGACGGCATAACGAGATGATTGTTATACGTGGAGTTCAGACGTGTG
Miseq_primer 12	CAAGCAGAAGACGGCATAACGAGATTCAGCGAAGTACTGGAGTTCAGACGTGTG
Miseq_primer 13	CAAGCAGAAGACGGCATAACGAGATGTCAAGTTGTGACTGGAGTTCAGACGTGTG
Miseq_primer 14	CAAGCAGAAGACGGCATAACGAGATAGGATGTGGTACTGGAGTTCAGACGTGTG
Miseq_primer 15	CAAGCAGAAGACGGCATAACGAGATCATTCCGAGTACTGGAGTTCAGACGTGTG
Miseq_primer 16	CAAGCAGAAGACGGCATAACGAGATACATCCTTGTGACTGGAGTTCAGACGTGTG
Miseq_primer 17	CAAGCAGAAGACGGCATAACGAGATTCGTGTGCGTACTGGAGTTCAGACGTGTG
Miseq_primer 18	CAAGCAGAAGACGGCATAACGAGATTCGCCAGAGTACTGGAGTTCAGACGTGTG
Miseq_primer 19	CAAGCAGAAGACGGCATAACGAGATTCGCTATGGTACTGGAGTTCAGACGTGTG
Miseq_primer 20	CAAGCAGAAGACGGCATAACGAGATGGCTCCTGGTACTGGAGTTCAGACGTGTG
Miseq_primer 21	CAAGCAGAAGACGGCATAACGAGATATCCGACAGTACTGGAGTTCAGACGTGTG
Miseq_primer 22	CAAGCAGAAGACGGCATAACGAGATAACATAATGTGACTGGAGTTCAGACGTGTG
Miseq_primer 23	CAAGCAGAAGACGGCATAACGAGATATGGTAGGGTACTGGAGTTCAGACGTGTG
Miseq_primer 24	CAAGCAGAAGACGGCATAACGAGATGCTAAGTAGTACTGGAGTTCAGACGTGTG
Miseq_primer 25	CAAGCAGAAGACGGCATAACGAGATACTTCTCTGACTGGAGTTCAGACGTGTG
Miseq_primer 26	CAAGCAGAAGACGGCATAACGAGATTAGATCCTGTGACTGGAGTTCAGACGTGTG
Miseq_primer 27	CAAGCAGAAGACGGCATAACGAGATTTACTGTCGTGACTGGAGTTCAGACGTGTG
Miseq_primer 28	CAAGCAGAAGACGGCATAACGAGATGGCATAGGGTACTGGAGTTCAGACGTGTG
Miseq_primer 29	CAAGCAGAAGACGGCATAACGAGATCAAGGCGAGTACTGGAGTTCAGACGTGTG
Miseq_primer 30	CAAGCAGAAGACGGCATAACGAGATGACGCTATGTGACTGGAGTTCAGACGTGTG
Miseq_primer 31	CAAGCAGAAGACGGCATAACGAGATAAGGCGACGTACTGGAGTTCAGACGTGTG

Miseq_primer 32	CAAGCAGAAGACGGCATAACGAGATCCTAGAATGTGACTGGAGTTCAGACGTGTG
Miseq_primer 33	CAAGCAGAAGACGGCATAACGAGATTGGTAACGGTGACTGGAGTTCAGACGTGTG
Miseq_primer 34	CAAGCAGAAGACGGCATAACGAGATCATCAGACGTGACTGGAGTTCAGACGTGTG
Miseq_primer 35	CAAGCAGAAGACGGCATAACGAGATGTGCGTAAGTGACTGGAGTTCAGACGTGTG
Miseq_primer 36	CAAGCAGAAGACGGCATAACGAGATCTATTCAAGTGACTGGAGTTCAGACGTGTG
Miseq_primer 37	CAAGCAGAAGACGGCATAACGAGATAGTGTCTTGTGACTGGAGTTCAGACGTGTG
Miseq_primer 38	CAAGCAGAAGACGGCATAACGAGATCCTTGCTGGTGACTGGAGTTCAGACGTGTG
Miseq_primer 39	CAAGCAGAAGACGGCATAACGAGATTTGCTGGAGTGACTGGAGTTCAGACGTGTG
Miseq_primer 40	CAAGCAGAAGACGGCATAACGAGATAGCTCTGGGTGACTGGAGTTCAGACGTGTG
Miseq_primer 41	CAAGCAGAAGACGGCATAACGAGATACCAAGGAGTGACTGGAGTTCAGACGTGTG
Miseq_primer 42	CAAGCAGAAGACGGCATAACGAGATGATAACCTGTGACTGGAGTTCAGACGTGTG
Miseq_primer 43	CAAGCAGAAGACGGCATAACGAGATTAGATGACGTGACTGGAGTTCAGACGTGTG
Miseq_primer 44	CAAGCAGAAGACGGCATAACGAGATTGCGAAGGGTGACTGGAGTTCAGACGTGTG
Miseq_primer 45	CAAGCAGAAGACGGCATAACGAGATGACCGAGAGTGACTGGAGTTCAGACGTGTG
Miseq_primer 46	CAAGCAGAAGACGGCATAACGAGATCAGACAATGTGACTGGAGTTCAGACGTGTG
Miseq_primer 47	CAAGCAGAAGACGGCATAACGAGATCTAGGTTCTGACTGGAGTTCAGACGTGTG
Miseq_primer 48	CAAGCAGAAGACGGCATAACGAGATGTTTCATTAGTGACTGGAGTTCAGACGTGTG
Miseq_primer 49	CAAGCAGAAGACGGCATAACGAGATAATGCGTTGTGACTGGAGTTCAGACGTGTG
Miseq_primer 50	CAAGCAGAAGACGGCATAACGAGATGAGAGTTGGTGACTGGAGTTCAGACGTGTG
Miseq_primer 51	CAAGCAGAAGACGGCATAACGAGATGATTACAGGTGACTGGAGTTCAGACGTGTG
Miseq_primer 52	CAAGCAGAAGACGGCATAACGAGATTGTGCTTAGTGACTGGAGTTCAGACGTGTG
Miseq_primer 53	CAAGCAGAAGACGGCATAACGAGATAGAACATTGTGACTGGAGTTCAGACGTGTG
Miseq_primer 54	CAAGCAGAAGACGGCATAACGAGATTACCGCTGGTGACTGGAGTTCAGACGTGTG
Miseq_primer 55	CAAGCAGAAGACGGCATAACGAGATTCCTGGTCTGACTGGAGTTCAGACGTGTG
Miseq_primer 56	CAAGCAGAAGACGGCATAACGAGATCCTGGATAGTGACTGGAGTTCAGACGTGTG
Miseq_primer 57	CAAGCAGAAGACGGCATAACGAGATATACCTGTGTGACTGGAGTTCAGACGTGTG
Miseq_primer 58	CAAGCAGAAGACGGCATAACGAGATAATGTTGGGTGACTGGAGTTCAGACGTGTG

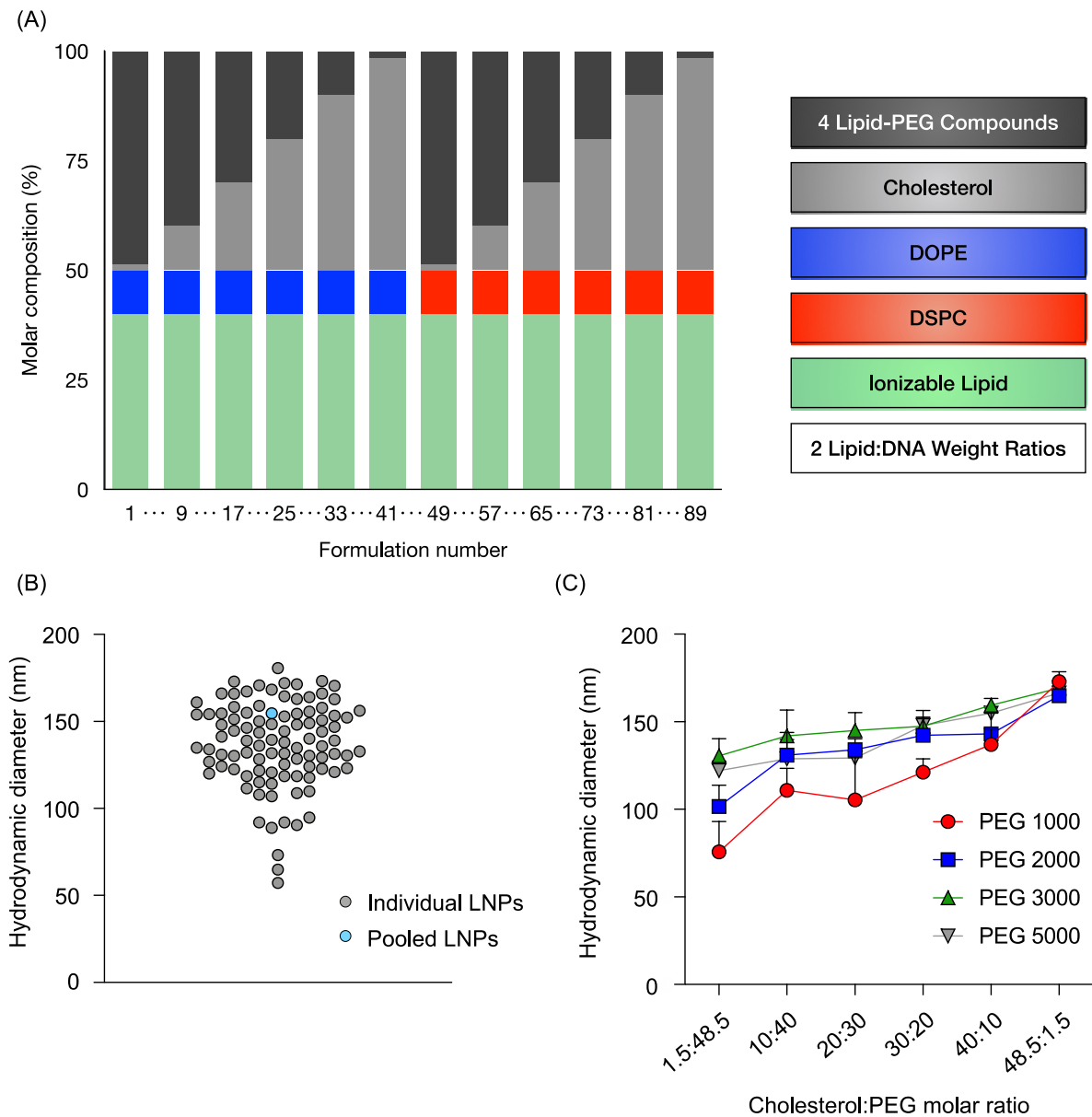


Figure S7. LNPs formulated by pipette mixing varied in size from 50 nm to 200 nm. (A) LNPs were formulated with 1 ionizable lipid (C12-200), 6 different excipient molar ratios, 2 different ionizable lipid:b-DNA weight ratios, 2 different helper lipids, and 4 different lipid-anchored polyethylene glycol (PEG) conjugates. Details on specific excipient molar ratios for each LNP are provided in **Table S1**. 94 out of 96 formulations formed stable LNPs based on DLS data. (B-C) LNP formulations were measured for hydrodynamic diameter by dynamic light scattering (DLS). (B) Individual LNPs and the uninjected pool were analyzed. (C) LNPs were analyzed based on their cholesterol to lipid-PEG molar ratio and their PEG molecular weight.

References

- [1] K. T. Love, K. P. Mahon, C. G. Levins, K. A. Whitehead, W. Querbés, J. R. Dorkin, J. Qin, W. Cantley, L. L. Qin, T. Racie, M. Frank-Kamenetsky, K. N. Yip, R. Alvarez, D. W. Y. Sah, A. De Fougérolles, K. Fitzgerald, V. Koteliansky, A. Akinc, R. Langer, D. G. Anderson, *Proc. Natl. Acad. Sci. U. S. A.* **2010**, *107*, 1864.
- [2] T. Wang, Y. Long, L. Liu, X. Wang, V. S. J. Craig, G. Zhang, G. Liu, *Langmuir* **2014**, *30*, 12850.
- [3] I. Reviakine, D. Johannsmann, R. P. Richter, *Anal. Chem.* **2011**, *83*, 8838.
- [4] D. Johannsmann, I. Reviakine, R. P. Richter, *Anal. Chem.* **2009**, *81*, 8167.
- [5] M. M. Billingsley, N. Singh, P. Ravikumar, R. Zhang, C. H. June, M. J. Mitchell, *Nano Lett.* **2020**, *20*, 1578.
- [6] J. A. Jackman, M. C. Kim, V. P. Zhdanov, N. J. Cho, *Phys. Chem. Chem. Phys.* **2016**, *18*, 3065.